J. Fluid Mech. (1984), *vol.* 141, *pp.* 431–453
Printed in Great Britain

Topographically generated cyclonic disturbance and lee waves in a stratified rotating fluid

By H. K. CHENG, H. HEFAZI
Department of Aerospace Engineering, University of Southern California, Los Angeles, California 90089–1454
AND S. N. BROWN
Department of Mathematics, University College London, England

(Received 13 December 1982 and in revised form 27 December 1983)

The flow about an obstacle in horizontal motion relative to a stratified Boussinesq fluid in a deep, rapidly rotating container is studied. Numerical and asymptotic analyses of the linearized boundary-value problems for a shallow topography are made to delineate the influence of stratification and ground topography on wave and flow structure, and to ascertain the presence of a solitary anticyclonic, or cyclonic, disturbance in the far field at high as well as low stratification. Although the analyses are restricted to the rapidly rotating case corresponding to a vanishingly small Rossby number, it is pointed out that the cyclonic feature remains a valid inviscid description in the far field except for an infinite Rossby number corresponding to no rotation.

1. Introduction

Wave and flow patterns produced by topographical features at the base of a rotating stratified fluid are intrinsically important to the dynamics of ocean and atmosphere, and to an understanding of the cyclogenesis in particular (Buzzi & Tibaldi 1977; Smith 1979*a*, *b*, *c*; Hogg 1980). This paper presents a study of the flow structure above an obstacle in a rapidly rotating fluid which has a vertical rotation axis and is linearly and stably stratified.

When the flowfield is considered as a dispersive medium for wave propagation, disturbances at large distances from a forcing region may be studied with the help of the group-velocity concept, corresponding to the Kelvin stationary-phase method (Lighthill 1965, 1978; Whitham 1974); the method has been powerfully illustrated by Lighthill (1978) in a number of problems of rotating and stratified fluids. The idea was subsequently applied by Redekopp (1975) in a study of a rapidly rotating fluid which is also stably stratified. Cheng (1977) analysed the flow pattern in a deep rotating container produced by the transverse uniform motion of an obstacle as a boundary-value problem at a low Rossby number, i.e. $\mathscr{R} \equiv u_c/\Omega_c L \ll 1$, where u_c and L are respectively the velocity and transverse lengthscales of the obstacle, and Ω_c is the angular velocity of the undisturbed rotating fluid. The reduced (outer) problem was solved for a thin three-dimensional obstacle in an unbounded (rotating) fluid. The wave pattern brought out are found to be consistent with Lighthill's theory, but the lee waves in Cheng's far-field solution do not appear to diminish far downstream. The discrepancy is resolved more recently in Cheng & Johnson (1982), where the asymptotic far field is also shown to be sensitively dependent on the topographical details, as is confirmed by numerical examples.

The container depth has been known to exert a pronounced influence on the results of rotating-fluid experiments (Hide, Ibbetson & Lighthill 1968). For a deep rotating container of height H, the parameter controlling the depth effect is $\Theta \equiv \mathscr{R}H/L$, irrespective of the obstacle thickness ratio (Cheng 1977). The reduced problems for finite Θ are investigated in Stewartson & Cheng (1979), where the linearized solutions for thin obstacles reveal several distinct features absent in the case of unbounded Θ. The study is extended to a viscous rotating flow in Johnson (1982). Interestingly, Johnson finds that the linearized solution for a thin two-dimensional obstacle also applies with equal validity to a *thick* ridge – irrespective of viscosity (as well as stratification), as long as the Rossby number is negligibly small.

Topographically generated inertial-wave patterns in a deep rotating annulus has been studied in the laboratory by Maxworthy (1977) (cf. the discussion in Stewartson & Cheng 1979) and by Heikes & Maxworthy (1982). In the latter work, linear analysis for a non-vanishing Rossby number is also presented; good agreement between theory and experiment in the streamline pattern above the ridges is apparent in a number of cases.

The present work extends the studies of Cheng (1977), Stewartson & Cheng (1979) and Cheng & Johnson (1982) to a rotating linearly stratified fluid with the aim of providing a more concrete description of the near and far fields than that via the group-velocity approach. An outstanding feature to be brought out below is the presence of an anticyclonic or cyclonic disturbance in the far field, depending on the topography. This feature coexists with the familiar inertial lee waves at all levels of stratification, except in the homogeneous case. Following Lighthill (1965, 1978) and Hide (1971), we view the flow structure analysed as an outward manifestation of a Proudman–Taylor column, and will accordingly place the emphasis on the far field of an unbounded fluid at a low Rossby number. A forthcoming paper will treat the corresponding problem for a non-vanishing $\mathscr{R}$, including the non-rotating limit $\mathscr{R} \to \infty$.

An earlier study of relevance to the present work is the group-velocity analysis of stratified rotating fluid by Redekopp (1975), which shows that the tilting angle of the inertial-wave caustic is proportional to a Brunt–Väisälä frequency. The tilting would, however, render the far field virtually free of disturbance in a strongly stratified case. This implication is at variance with the theory of Hogg (1973) on quasi-geostrophic flow near a hydrostatic balance, as well as analyses of the geostrophic and related models of planetary atmosphere by Ingersoll (1969), Huppert (1975), Buzzi & Tibaldi (1977), Johnson (1978), Smith (1979*b*, *c*) and Hogg (1980). These works lead to a Laplace equation governing the flow above a submerged obstacle, which is also noted independently by Cheng (1977). On the other hand, the domain of applicability of the Laplace equation is not at all apparent, as exemplified by the bluff body considered in Hogg's original study, which does not meet the implicit requirements of a thin obstacle. The desire to clarify these ambiguities provide motivation for the present work. The results of the analysis should enhance our understanding of how a stable stratification manifests itself in the rotating fluid, and the manner of transition between the homogeneous and a strongly stratified limit. In passing, we note that the linearized boundary-value problem of the rotating Boussinesq fluid has been analysed for two-dimensional ridge-like topography earlier by Queney (1948) and more recently by Smith (1979*a*, *b*, *c*). The significant manifestation of the stratification in the far field (cf. §5.3) has not been thoroughly studied therein.

As an example of wave propagation in a dispersive medium, the present study

illustrates the need for an amendment of the stationary-phase and group-velocity methods. These methods do not take into account the contribution from the *evanescent* components of the propagating wavetrain; the latter attenuates in a certain (outward) direction (cf. Stix 1962, p. 13) and may be referred to also as trapped waves (see Lighthill 1978, pp. 302–308). These components decay with distance generally at an exponential rate, but an exception must be made for the vanishing of the rate at an *isolated* (horizontal) wavenumber (beyond the cut-off), where the phase is also *singular*. It is this exception that gives rise to the distinct anticyclonic, or cyclonic, far-field structure upstream as well as downstream, unaccountable by either a group-velocity analysis or the steepest-descent method. Since the sense of rotation in the flow feature in question can be either cyclonic or anticyclonic, depending on the sign of the displacement volume of the topography, we shall use 'cyclonic' as a descriptive for the type of features wherever the distinction between the two becomes unnecessary.

The linear system studied in detail in §5 is recognized as a form of the inertial wave equation of a rotating flow generalized to a Boussinesq fluid, which is also familiar in meteorological and oceanographical literature (see e.g. Eckart 1969; Ogura & Phillips 1962; Blumen 1972). Instead of beginning with the familiar equation last mentioned, we consider the problem at hand as one describing the flows in an upright, deep, rapidly rotating container, of which the analysis can be subject to verification in a laboratory experiment. We shall set down first in §§3 and 4 the equations reduced for a *low* Rossby number without the assumption of a thin obstacle. This will allow us to focus on the more essential part of the original equations under $\mathscr{R} \ll 1$. The subsequent linearization for thin obstacles yields solutions which may then serve as examples possessing the same (length)scales and occupying the same spatial and parameter domains as do the nonlinear solutions for the thick obstacles. Several resultant features, including the cyclonic disturbance in the far field, are expected to remain also for an isolated thick obstacle. The results should be very useful for the nonlinear analysis of the reduced problem to follow. Thus the present approach of first presenting the reduced problem without linearization in §§3 and 4 is believed to represent a rational step. In this connection, we point out that, under the quasi-geostrophy ($\mathscr{R} \ll 1$), the linear system is applicable also to a *thick* two-dimensional ridge, and that the equation governing the vertical velocity component in a highly stratified case is not always linearizable as is the pressure equation.

In §2 the assumption and the analytical framework are stated more concisely; the basic scales and parameters will be defined, and the domains of interest will be indicated. The linearized reduced equations for a thin obstacle, specialized for an unbounded Θ, is analysed in §5, where flow and wave patterns at various degrees of stratification are delineated and their crucial far-field behaviour is described. Section 6 presents numerical examples of the linear solution computed from a fast-Fourier-transform (FFT) algorithm at different reduced heights and degrees of stratification; their comparison with the far-field analysis substantiates the presence and the relative importance of the cyclonic disturbance at most levels of stratification. Analytical details and discussions omitted below are more fully presented in (Cheng, Hefazi & Brown 1983).

2. Assumptions and parameter domains

We consider the perturbation of a stably stratified inviscid fluid that is otherwise in a state of rigid-body rotation about a vertical axis at a uniform angular velocity

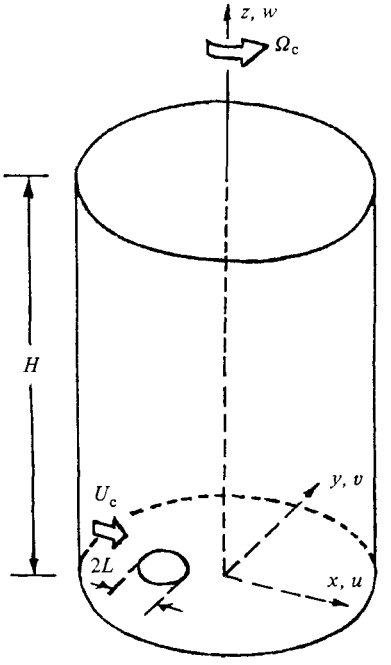

FIGURE 1. Illustration of coordinates and notations used in the analysis of fluid motion produced by a body moving in a transverse plane within a rotating vessel.

Ω_c. A Cartesian coordinate system (x, y, z) fixed to the *undisturbed* rotating fluid is adopted, where z measures the distance upward along a vertical axis. The components of the perturbation velocity corresponding to x, y and z are denoted by u, v and w. The fluid dynamics to be analysed results from the slow, horizontal relative motion of an impermeable obstacle or topography at the base, $z = 0$, which has a typical velocity u_c (cf figure 1). The obstacle is assumed to move from left to right in the direction of increasing x. An upper impermeable boundary is assumed at $z = H$. The horizontal extent of the field of interest is assumed to be large enough that sidewall effects are not considered.

A linear form of the density variation in the undisturbed fluid, namely that in a Boussinesq fluid (Yih 1965), is adopted. More specifically

$$\frac{\rho_e - \rho_0}{\rho_0} = -\frac{\epsilon}{H} z, \tag{2.1}$$

where ρ_e is the equilibrium density and ρ_0 is the density at the base; only positive values of ϵ/H are considered.† The most important parameter controlling the stratification effect in the present study is

$$\theta \equiv g \frac{\epsilon}{H} \frac{L^2}{u_c^2}, \tag{2.2a}$$

† With the centrifugal acceleration, the Boussinesq-fluid assumption must be corrected to account for the departure of the constant equilibrium density surface from a horizontal plane. This effect is estimated to be not large, at least in several existing laboratory facilities (cf. Cheng *et al.* 1982).

which is independent of Ω_c, even though the rotation is a basic ingredient of the present problem. Noting that $N \equiv (g\epsilon/H)^{\frac{1}{2}}$ is the Brunt–Väisälä frequency, θ is seen to be simply the inverse square of a Froude number u_c/NL (Yih 1978, p. 232)

$$\theta = \left(\frac{NL}{u_c}\right)^2. \tag{2.2b}$$

For a small or unit-order θ, the length and velocity scales employed in Cheng (1977) or Stewartson & Cheng (1979) for the principal flow region above the obstacle will be adequate. At a high stratification, the appropriate velocity scale is, instead of u_c, $u_s \equiv \tau NL$ (τ being the obstacle thickness), and the proper axial lengthscale is, instead of $L/\mathscr{R}$, Ω_c/LN or $L/\theta^{\frac{1}{2}}\mathscr{R}$. It follows that the proper depth parameter at a high θ should be $\Theta_s \equiv NH/\Omega_c L = \theta^{\frac{1}{2}}\Theta$.

The combinations of the intermediate and limiting values of $\mathscr{R}$, θ, Θ etc. give rise to a variety of distinct domains of this inviscid, rotating, stratified fluid. Although the present paper is limited mainly to $\mathscr{R} \to 0$, both moderate and strong stratification ($\theta = O(1)$ and $\theta \gg 1$) are considered. In terms of the foregoing parameters, the results of the formulation for the moderately stratified case may be identified with the single limit

$$\mathscr{R} \to 0; \quad \Theta, \theta, \tau \text{ fixed}; \tag{2.3}$$

and that, for the strongly stratified case ($\theta \gg 1$), the analysis may be identified with the (single) limit

$$\mathscr{R} \to 0; \quad \Theta_s, \theta\mathscr{R}^2, \tau \text{ fixed}. \tag{2.4}$$

The limit (2.3) can be relaxed to include special cases with an unbounded Θ, also (vanishingly) small θ and small τ; similarly, unbound Θ_s, small θ^2 can be shown to be included in (2.4).† For problems of the Earth's atmosphere the domain $(N/\Omega_c)^2 = \theta\mathscr{R}^2 \gg 1$ is important. The limit $\theta\mathscr{R}^2 \to \infty$, i.e. $\theta \gg \mathscr{R}^{-2} \gg 1$, will be considered along with a non-vanishing $\mathscr{R}$ in a subsequent work.

The linearized equations for the pressure disturbance (of §§ 3.3 and 3.5) result from a small thickness ratio τ in (2.3) and (2.4). The examples analysed in detail in §5 correspond to unbounded Θ and Θ_s, in addition to a vanishingly small τ. It is essential to point out that the limit $\tau \to 0$ and $\Theta \to \infty$, or $\Theta_s \to \infty$, do not lead to degeneracy of the reduced equations. In passing, one may note that the nonlinear convective contribution has a relative order of magnitude of $\tau\theta^{\frac{1}{2}}$, or $\tau\mathscr{R}^{-1}$, under limit (2.4); thus the formulation in the asymptotic theory would have to distinguish a bounded from an unbounded $\tau\theta^{\frac{1}{2}}$. However, except for a different error estimate, the reduced equations for moderate and large $\tau\theta^{\frac{1}{2}}$ are found to be completely equivalent.

3. Horizontally moving obstacle in a stratified, rapidly rotating fluid: asymptotic theory for finite θ

We follow Cheng (1977) in the normalization of t, x, y, z, u, v, w and p by L/u_c, L, L, L, τu_c, τu_c, τu_c and $\tau\rho\Omega_c u_c L$ respectively. A slight departure from that of Cheng is the introduction of τ in the velocity and pressure scale to reflect the thickness influence. Absent from Cheng's (1977) work is the density perturbation from its equilibrium value, denoted here by ρ, which will be normalized by $\tau\epsilon\rho_0 L/H$. We also rescale the vertical distance in the region of interest by $L/\mathscr{R}$, instead of L; this dimensionless outer variable will be denoted by $\tilde{z}$.

† Note that a fixed $\theta\mathscr{R}^2$ in (2.4) implies $1 \ll \theta = O(\mathscr{R}^{-2})$, and a small $\theta\mathscr{R}^2$ means $1 \ll \theta \ll \mathscr{R}^{-2}$.

3.1. *Equations governing the principal flow region*

The need of the variable $\tilde{z} \equiv \mathscr{R}z/L$ is apparent from the well-known error estimate supporting the Proudman–Taylor theorem. Namely, $\partial p/\partial z, \partial u/\partial z$ etc. $= O(\mathscr{R})$ in regions not far from the obstacle; therefore the theorem must break down at a distance $z = O(\mathscr{R}^{-1})$. In this range of $\tilde{z}$, referred to as the outer region in Cheng (1977), the partial differential equations governing the dynamics of a rapidly rotating inviscid fluid, initially stratified according to (2.1), can be simplified to

$$\left.\begin{gathered} -2v+\frac{\partial p}{\partial x}=0, \quad 2u+\frac{\partial p}{\partial y}=0, \quad \frac{\partial p}{\partial \tilde{z}}+\frac{\mathrm{D}'}{\mathrm{D}t}w+\theta\rho=0, \\ 2\frac{\partial w}{\partial \tilde{z}}-\frac{\mathrm{D}'}{\mathrm{D}t}\zeta=0, \quad \frac{\mathrm{D}'}{\mathrm{D}t}\rho-w=0, \end{gathered}\right\} \tag{3.1}$$

where $\mathrm{D}'/\mathrm{D}t$ is a convective derivative and ζ is the horizontal vorticity:

$$\frac{\mathrm{D}'}{\mathrm{D}t} \equiv \frac{\partial}{\partial t}+\tau\left(u\frac{\partial}{\partial x}+v\frac{\partial}{\partial y}\right), \quad \zeta \equiv \frac{\partial v}{\partial x}-\frac{\partial u}{\partial y}.$$

With the stipulation that all variables are of unit order in this region and that θ is finite, terms omitted from (3.1) belong to an order $\mathscr{R}$ higher. Equation (3.1) admits expansions in small $\tilde{z}$, which confirms the existence of a columnar (inner) region next to the obstacle, and yields the inner boundary conditions for the solution

$$w = \frac{\mathrm{D}'}{\mathrm{D}t}Z_w(x, y, t) \quad \text{as} \quad \tilde{z} \to 0. \tag{3.2a}$$

Similarly, one has the condition on the upper boundary

$$w = 0 \quad \text{at} \quad \tilde{z} = \Theta. \tag{3.2b}$$

A simplification in the problem formulation has been gained through the matching with the inner columnar structure, whereby the formulation permits the transfer of the boundary condition from the body surface to the horizontal plane $\tilde{z} = 0$ without the assumption of a thin obstacle, subject to a relative error of the order $\mathscr{R}$. At a large lateral distance $(x^2+y^2)^{\frac{1}{2}} \gg 1$ all five perturbation variables are assumed to vanish.

For the case of an unbounded Θ of interest, the requirement for perturbation quantities to vanish in the far field will not suffice. We shall impose, in this case, a radiation condition corresponding to a non-negative (time average) energy flux directed towards infinity. This will correspond to ruling out all incoming propagating waves under $\mathscr{R} \to 0$ (see §5.1).

The first two equations of (3.1) show that the flow is nearly geostrophic, but the final determination depends crucially on the inertial corrections to the two geostrophic relations, which lead to the fourth equation of (3.1) and is responsible for the inertial waves. Equations (3.1) are generally *nonlinear*; the problem may be further complicated by the appearance of the Taylor-column wall in the vicinity of a bluff obstacle, which is expected to give rise to a ring of singularities, and thus a non-uniformity, in the solution to (3.1) at $\tilde{z} = 0$.

3.2. *The linearized problem*

In this paper we shall mainly be concerned with examples involving thin obstacles ($\tau \ll 1$). Except for a modification brought about by a change in the equivalent

obstacle shape due to the nonlinearity in the near field, the three-dimensional far field determined by the linear theory should not differ substantially from that for a thick obstacle.

In the (second) limit $\tau \to 0$, $\mathrm{D}'/\mathrm{D}t$ in (3.1) becomes $\partial/\partial t$, (3.1) may then be linearized and combined to yield, with $\nabla_\perp^2 \equiv \partial^2/\partial x^2 + \partial^2/\partial y^2$,

$$\frac{\partial}{\partial t}\left[4\frac{\partial^2}{\partial \tilde{z}^2} + \left(\frac{\partial^2}{\partial t^2} + \theta\right)\nabla_\perp^2\right] p = 0, \tag{3.3}$$

and (3.2) may be replaced by

$$\frac{\partial}{\partial t}\left[\frac{\partial p}{\partial \tilde{z}} + \left(\frac{\partial^2}{\partial t^2} + \theta\right) Z_w\right] = 0 \quad \text{at} \quad \tilde{z} = 0, \tag{3.4a}$$

$$\frac{\partial}{\partial t}\frac{\partial p}{\partial \tilde{z}} = 0 \quad \text{at} \quad \tilde{z} = \Theta, \tag{3.4b}$$

where, as before, (3.4*b*) will be replaced by a radiation condition if Θ is unbounded. The vanishing of the disturbance at $x^2 + y^2 \to \infty$ is also assumed.

Equation (3.3) represents an extension of the familiar inertial wave equation (see e.g. Greenspan 1969; Lighthill 1978) to a stratified fluid, taking into account the influence of the displaced constant-density surfaces; (3.3) may therefore be referred to as the (linear) equation of *inertial–baroclinic waves*. A more complete form of the linearized equation allowing non-vanishing $\mathscr{R}$ and θ can be derived quite readily from the conservation of potential vorticity in the context of a global model of planetary atmosphere (see Blumen 1972); its equivalence to (3.3) in the flow region $\tilde{z} = O(1)$ under the limit (2.3) can be readily checked. Interestingly, following the thrust of Obukhov (1949), Blumen (1972) indicates how a quasi-geostrophic system equivalent to (3.3) may also be derived from an analysis with multiple timescales.

Since the *far-field* flow pattern of a steadily moving obstacle is the focus of the present study, we shall obtain explicit solutions to (3.3), (3.4*a*) for an unbounded fluid, taking Z_w in the form of $Z_w(x-t, y)$ pertaining to a steadily moving obstacle. The solution structure will be delineated both asymptotically (for large $\tilde{z}$) and numerically.

Equations (3.1), (3.2) and (3.3), (3.4) provide a suitable framework for the study of departure from the inertial-wave domain, but the ordering implicit in the formulation for the limit $\mathscr{R} \to 0$ may become inappropriate as θ increases beyond order unity. A reformation based on a different set of variables allowing an unbounded θ is therefore presented below.

4. Hydrostatic balance as a limit of a strongly stratified, rotating fluid: asymptotic theory for high θ

An examination of the dependence on θ in the equations of §3 indicate that, as θ increases to beyond unit order, the normalized perturbations p, u, v and ζ would increase like $\theta^{\frac{1}{2}}$, while the vertical variable $\tilde{z}$ should be rescaled as $\theta^{\frac{1}{2}}z$. In the following, we will present the governing equations first for the domain $1 \ll \theta \ll \mathscr{R}^{-2}$. Subsequently we will examine a more strongly stratified domain $1 \ll \theta = O(\mathscr{R}^{-2})$. As previously mentioned, the range of a still higher θ, namely $\theta \gg \mathscr{R}^{-2}$, will not be considered.

As will be apparent later, the magnitudes of w and $\mathrm{D}/\mathrm{D}t$ belong to $O(\tau\theta^{\frac{1}{2}})$. Therefore, in order to provide an unambiguous formulation of the reduced problem,

one should establish the reduced equation systems for the bounded and unbounded $\tau\theta^{\frac{1}{2}}$ separately; these have been documented in Cheng *et al.* (1982). In the following, we shall formulate the problem in the principal flow region under $\tau\theta^{\frac{1}{2}} = O(1)$, and will only remark briefly later on the case $\tau\theta^{\frac{1}{2}} \gg 1$, since the two reduced systems turn out to be equivalent.

4.1. *The problem for* $1 \ll \theta \ll \mathscr{R}^{-2}$

We introduce the rescaled variables for p, u and v:

$$\left.\begin{aligned} \tilde{p} \equiv \frac{p}{\theta^{\frac{1}{2}}} = \frac{p^*-p_e^*}{\rho\Omega_c u_s L}, \\ \tilde{u} \equiv \frac{u}{\theta^{\frac{1}{2}}} = \frac{u^*}{u_s}, \quad \tilde{v} \equiv \frac{v}{\theta^{\frac{1}{2}}} = \frac{v^*}{u_s}, \end{aligned}\right\} \tag{4.1}$$

where u_s is a reference velocity independent of u_c and Ω_c:

$$u_s \equiv \tau\theta^{\frac{1}{2}}u_c = \tau\left(\epsilon\frac{L}{H}gL\right)^{\frac{1}{2}}.$$

With the variables introduced in (4.1), and replacing $\tilde{z}$ by $\tilde{z}' \equiv \theta^{\frac{1}{2}}\mathscr{R}\tilde{z} = \theta^{\frac{1}{2}}\tilde{z}$, the inviscid equations for the flow region of interest become

$$\left.\begin{aligned} -2\tilde{v}+\frac{\partial\tilde{p}}{\partial x} = 0, \quad 2\tilde{u}+\frac{\partial\tilde{p}}{\partial y} = 0, \quad \frac{\partial\tilde{p}}{\partial\tilde{z}'}+\rho = 0, \\ 2\frac{\partial w}{\partial\tilde{z}'}-\frac{\mathrm{D}'}{\mathrm{D}t}\zeta = 0, \quad \frac{\mathrm{D}'}{\mathrm{D}t}\rho-w = 0, \end{aligned}\right\} \tag{4.2}$$

where

$$\frac{\mathrm{D}'}{\mathrm{D}t} \equiv \frac{\partial}{\partial t}+\tau\theta^{\frac{1}{2}}\left(\tilde{u}\frac{\partial}{\partial x}+\tilde{v}\frac{\partial}{\partial y}\right).$$

The relative errors in (4.2) are, at the most (Cheng *et al.* 1982),

$$\epsilon_1 = O(\theta^{-1}, \theta^{\frac{1}{2}}\mathscr{R}).$$

It follows that, under $1 \ll \theta \ll \mathscr{R}^{-2}$, and $\tau\theta^{\frac{1}{2}} = O(1)$, the quasi-geostrophic flow approaches a hydrostatic balance in the vertical momentum equation, yet the baroclinic effects are still crucial for this system. A consequence of (4.2) will be deduced in §4.2. It is essential to note that the assumption of a thin obstacle is implicit, since $1 \ll \theta \ll \mathscr{R}^{-2}$ and $\tau\theta^{\frac{1}{2}} = O(1)$ require $\tau \ll 1$.

The solution admits a Taylor expansion in $\tilde{z}'$, which confirms the existence of an inner columnar structure over $\mathscr{R}\theta^{\frac{1}{2}} \ll \tilde{z}' \ll 1$, and identifies the boundary condition for the solution to (4.2) to be

$$w = \frac{\mathrm{D}'}{\mathrm{D}t}Z_w(x, y, t) \quad \text{as} \quad \tilde{z}' \to 0. \tag{4.3}$$

The matching also determines $\tilde{p}$, $\tilde{u}$, $\tilde{v}$, $\tilde{\zeta}$ and $\tilde{\rho}$ on the obstacle in terms of their values in the inner limit $\tilde{z}' \to 0$, with errors again comparable to ϵ_1. Similarly, the upper boundary condition is

$$w = 0 \quad \text{for} \quad \tilde{z}' = \theta^{\frac{1}{2}}\mathscr{R}\frac{H}{L} = \theta^{\frac{1}{2}}\Theta \equiv \Theta_s. \tag{4.4}$$

At large lateral distance $x^2+y^2 \to \infty$ we assume all disturbances to subside, and in the unbounded case $\Theta_s \to \infty$ a radiation condition barring all measurable incoming disturbance will be enforced.

For an unbounded $\tau\theta^{\frac{1}{2}}$ the vertical velocity w and the time t should be rescaled as

$$\tilde{w} \equiv \frac{w}{\tau\theta^{\frac{1}{2}}}, \quad \tilde{t} \equiv \frac{\tilde{t}}{\tau\theta^{\frac{1}{2}}}. \tag{4.5}$$

With these modifications, the $\tilde{z}'$-derivatives of $\tilde{p}$, $\tilde{u}$, $\tilde{v}$, $\tilde{w}$ and also $\tilde{\rho}$ are seen to be of order $\theta^{\frac{1}{2}}\mathscr{R}$ or higher. The equations governing the region $\tilde{z}' = \theta^{\frac{1}{2}}\mathscr{R}z = O(1)$ in this case are reduced to a system which is again identifiable with (4.2)–(4.4) except for the replacement of w by $\tilde{w}$, and $\mathrm{D}'/\mathrm{D}t$ by $\mathrm{D}'/\mathrm{D}t \equiv \partial/\partial t + \tilde{u}\,\partial/\partial x + \tilde{v}\,\partial/\partial y$. The order θ^{-1} in the relative error in ϵ_1 is now to be replaced by τ^2, which results from the remainder in the hydrostatic balance. Therefore, taking into account both large and small $\tau\theta^{\frac{1}{2}}$, the error in (4.2) is parametrically

$$\epsilon_1' = O(\theta^{-1}, \theta^{\frac{1}{2}}\mathscr{R}, \tau^2). \tag{4.6}$$

The foregoing results can be extended to a still higher stratification with $\theta = O(\mathscr{R}^{-2})$, for which a distinct columnar inner region no longer exists since $\theta^{\frac{1}{2}}\mathscr{R} = O(1)$ and the principal (outer) region in which (4.2) applies is, in fact, $z = O(1)$. The *relative* errors of (4.2)–(4.4) in this case become $O(\mathscr{R}, \tau)$.

4.2. *Reduction to Laplace equation: thin obstacles*

The equations reduced in §4.1 are seen to hold only for a *thin* obstacle ($\tau \ll 1$) even though the systems under $1 \ll \theta \ll \mathscr{R}^{-2}$ and $1 \ll \theta = O(\mathscr{R}^{-2})$ remain nonlinear in general. However, the equation governing the pressure and the horizontal velocity fields can be reduced to a Laplace equation as follows.

The term $\partial\tilde{w}/\partial\tilde{z}'$ in the fourth equation of (4.2) may first be eliminated by differentiating the fifth equation of (4.2) with respect to $\tilde{z}'$ and then eliminating $\tilde{\rho}$ through the hydrostatic balance, so that

$$2\frac{\partial}{\partial\tilde{z}'}\frac{\mathrm{D}'}{\mathrm{D}t}\frac{\partial}{\partial\tilde{z}'}\tilde{p} + \frac{\mathrm{D}'}{\mathrm{D}t}\zeta = 0. \tag{4.7}$$

Thanks to the geostrophy which permits communication of operators $\partial/\partial\tilde{z}'$ and $\mathrm{D}'/\mathrm{D}t$ for $\partial\tilde{p}/\partial\tilde{z}'$, the equation governing $\tilde{p}$ in the leading order may finally be reduced from (4.7) to

$$\frac{\mathrm{D}'}{\mathrm{D}t}\left[\left(4\frac{\partial}{\partial\tilde{z}'^2} + \nabla_\perp^2\right)\tilde{p}\right] = 0. \tag{4.8}$$

Through (4.2), upper and lower boundary conditions may also be written in a Neumann form for $\tilde{p}$:

$$\frac{\mathrm{D}'}{\mathrm{D}t}\left[\frac{\partial}{\partial\tilde{z}'}\tilde{p} + Z_w\right] = 0 \quad \text{as} \quad \tilde{z}' \to 0, \quad \frac{\mathrm{D}'}{\mathrm{D}t}\frac{\partial}{\partial\tilde{z}'}\tilde{p} = 0 \quad \text{at} \quad \tilde{z} = \Theta_s. \tag{4.9a, b}$$

For a system in which the fluid can be assumed to originate from a uniform state far upstream where $Z_w \equiv 0$, the convective derivative may be dropped from both (4.8) and (4.9). After scaling out the factor 4, one arrives from (4.8) at the Laplace equation of Hogg (1973) with Neumann boundary conditions. We note that the equation governing the limit solution for $\tilde{w}$ cannot be linearized unless $\tau\theta^{\frac{1}{2}}$ is small.

An important conclusion reached from the above study is that the system (4.8), (4.9) is recoverable from the linearized system (3.3), (3.4), which is derived for a finite θ. Therefore the latter system may now be meaningfully applied to the study of transition between the homogeneous and the highly stratified limit, as will be carried out in §5.

In Hogg's (1973) analysis leading up to (4.8), the assumption $\Theta_s = O(1)$ and $\tau\theta^{\frac{1}{2}} = O(1)$ are implicit, although the requirement of $\tau \ll 1$ is not clearly pointed out.† In the unbounded case, the far-field pressure disturbance obeying (4.8) and (4.9a) will asymptotically approach

$$\tilde{p} \sim \frac{1}{\pi} \frac{\iint Z_w \,\mathrm{d}x\,\mathrm{d}y}{(x^2+y^2+(\frac{1}{2}\tilde{z}')^2)^{\frac{1}{2}}}, \tag{4.10}$$

where the surface integral of Z_w is the normalized displacement volume. The behaviour arrived here for a high θ signifies, via the quasi-geostrophy, an anticyclonic fluid motion above a compact topography when the displacement volume is positive and a cyclonic one when negative. This results in an asymmetrically disposed horizontal streamline pattern. A closed streamsurface is expected to form as $\tau\theta^{\frac{1}{2}}$ becomes of unit order; its horizontal extent and height increase with $\tau\theta^{\frac{1}{2}}$. On the other hand, (4.10) shows that the magnitudes of the horizontal velocities attenuate more rapidly than the pressure as $(\tilde{z}')^{-2}$; the vertical velocity w will decay even faster, as $(\tilde{z}')^{-3}$, since $w = \mathrm{D}'\rho/\mathrm{D}t = -\mathrm{D}'(\partial\tilde{p}/\partial\tilde{z}')/\mathrm{D}t$. Subsequent examples will show that the cyclonic disturbance corresponding to (4.10) remains a far-field feature for all $\theta \neq 0$. Buzzi & Tibaldi (1977) have studied effects of a higher-order inertial (finite $\mathscr{R}$) correction to Hogg's (1973) Laplace equation, i.e. (4.8).

5. Stationary flow pattern for an arbitrary topography: thin obstacle in a container of infinite depth

To exemplify more clearly the stratification effect on the inertial-wave field generated by an obstacle, the linearized system (3.3), (3.4) for a thin object is solved for the case of uniform translation in a container of infinite depth. The far field and the computed results deduced from the solution will illustrate the transition between the limits of the zero θ and an unbounded θ and will confirm the presence of the cyclonic disturbance for all $\theta \neq 0$.

5.1. *Solution in terms of obstacle geometry*

In the body-fixed coordinates (x', y, z) with $x' \equiv x - t$, (3.3) and (3.4a) may be written as

$$\left[\frac{\partial}{\partial\hat{z}^2} + \left[\left(\frac{\partial}{\partial t} - \frac{\partial}{\partial x'}\right)^2 + \theta\right]\nabla_\perp^2\right]\psi = 0, \tag{5.1}$$

$$\frac{\partial\psi}{\partial\hat{z}} = \left[\left(\frac{\partial}{\partial t} - \frac{\partial}{\partial x'}\right)^2 + \theta\right]Z_w \quad \text{at} \quad \hat{z} = 0, \tag{5.2}$$

where, for convenience, p and $\tilde{z}$ have been replaced by

$$\psi \equiv -\tfrac{1}{2}p, \quad \hat{z} \equiv \tfrac{1}{2}\tilde{z}$$

respectively. A radiation condition will be applied to the far field in addition to the assumption of a vanishing disturbance as $x'^2 + y^2 + \hat{z}^2 \to \infty$.

The solution ψ may be constructed from sinusoidal (exponential) wavetrains

$$\exp[\mathrm{i}(\omega x' + \sigma y + k\hat{z} - \Omega' t)],$$

with ω, σ, k and Ω' satisfying the dispersion relation of (5.1), which in the stationary case (i.e. $\Omega' \to 0$) gives

$$k = \pm|k| \quad \text{for} \quad \omega^2 > \theta, \quad k = \pm\mathrm{i}|k| \quad \text{for} \quad \omega^2 < \theta,$$

† Hogg's parameters S and β correspond to $2\pi\Theta_s$ and $\tau\theta^{\frac{1}{2}}/(2\pi)^{\frac{1}{2}}\Theta_s$ respectively. Hogg's (1980) $S\delta/\epsilon$ is identified here as $\tau\theta^{\frac{1}{2}}$.

with

$$|k| = |(\omega^2-\theta)(\omega^2+\sigma^2)|^{\frac{1}{2}}.$$

For the problem of $\mathscr{R}\to 0$ with a fixed θ, the radiation condition is equivalent to the exclusion of all incoming wavetrains in the (x, y, z, t)-frame, since the group and phase velocities have the same sign for the system at hand.† Since $x' = x-t$, the algebraic sign for k must be chosen to agree with that of ω so as to give outgoing wavetrains for $\omega^2 > \theta$. The condition also rules out disturbances with amplitudes increasing with $\hat{z}$; therefore only the positive imaginary root of k is admissible for $\omega^2 < \theta$. This corresponds to the *evanescent* waves. The above conclusions may be expressed more compactly by defining the function $(\omega^2-\theta)^{\frac{1}{2}}$ as

$$(\omega^2-\theta)^{\frac{1}{2}} = \begin{cases} +|\omega^2-\theta|^{\frac{1}{2}} & (\theta^{\frac{1}{2}} < \omega), \\ \mathrm{i}\,|\omega^2-\theta|^{\frac{1}{2}} & (-\theta^{\frac{1}{2}} < \omega < \theta^{\frac{1}{2}}), \\ -|\omega^2-\theta|^{\frac{1}{2}} & (\omega < -\theta^{\frac{1}{2}}). \end{cases} \tag{5.3}$$

The steady-state solution satisfying the radiation condition may now be represented by an integral over the (ω, σ)-domain:

$$\psi = \int_{-\infty}^{\infty}\int_{-\infty}^{\infty} h(\omega,\sigma)\exp[\mathrm{i}(\omega x' + \sigma y + (\omega^2-\theta)^{\frac{1}{2}}(\omega^2+\sigma^2)^{\frac{1}{2}}\hat{z})]\,\mathrm{d}\omega\,\mathrm{d}\sigma, \tag{5.4a}$$

where the function $h(\omega, \sigma)$ is determined from the inner boundary condition (5.2) as

$$h(\omega,\sigma) = \frac{\mathrm{i}F(\omega,\sigma)(\omega^2-\theta)^{\frac{1}{2}}}{(2\pi)^2(\omega^2+\sigma^2)^{\frac{1}{2}}}, \tag{5.4b}$$

with $F(\omega, \sigma)$ being the Fourier transform of $Z_w(x', y)$:

$$F(\omega,\sigma) \equiv \int_{-\infty}^{\infty}\int_{-\infty}^{\infty} Z_w(x', y)\,\mathrm{e}^{-\mathrm{i}\omega x' - \mathrm{i}\sigma y}\,\mathrm{d}x'\,\mathrm{d}y. \tag{5.4c}$$

For surfaces such as a spherical cap, or simple three-dimensional shapes with an algebraic or exponential decay, the integral of ψ exists in the Riemann sense; its computation amounts to the inversion of the Fourier transform $(2\pi)^2 h(\omega, \sigma)\,\mathrm{e}^{\mathrm{i}k\hat{z}}$ and can be computed efficiently via standard fast-Fourier-transform (FFT) techniques for each fixed $\hat{z}$. Results are discussed in §6.

Solution (5.4) can be written out as two distinct parts: one is made up of components of the outgoing, propagating (non-attenuating) wavetrains and the other is composed of the evanescent components. The latter attenuate as $\hat{z}\to\infty$ and hence can propagate only horizontally. Thus

$$\psi = \psi_1 + \psi_2,$$

$$\psi_1 \equiv \int_{-\infty}^{\infty}\mathrm{d}\sigma\int_{\theta^{\frac{1}{2}}}^{\infty} h(\omega,\sigma)\,\mathrm{e}^{\mathrm{i}\omega x' + \mathrm{i}\sigma y + \mathrm{i}|k|\hat{z}}\,\mathrm{d}\omega + \int_{-\infty}^{\infty}\mathrm{d}\sigma\int_{-\infty}^{-\theta^{\frac{1}{2}}} h(\omega,\sigma)\,\mathrm{e}^{\mathrm{i}\omega x' + \mathrm{i}\sigma y - \mathrm{i}|k|\hat{z}}\,\mathrm{d}\omega, \tag{5.5a}$$

$$\psi_2 \equiv \int_{-\infty}^{\infty}\mathrm{d}\sigma\int_{-\theta^{\frac{1}{2}}}^{\theta^{\frac{1}{2}}} h(\omega,\sigma)\,\mathrm{e}^{\mathrm{i}\omega x' + \mathrm{i}\sigma y - |k|\hat{z}}\,\mathrm{d}\omega. \tag{5.5b}$$

† The time-average energy of a wavetrain propagates in the direction of the group velocity (Lighthill 1965, 1978; Whitham 1973). The z-component of the group velocity for a plane wave in the present problem is $k/\omega(\omega^2+\sigma^2)$. The group and phase velocities have opposite signs if $\theta > 4\mathscr{R}^{-2}$.

For the outgoing wave portion ψ_1 the stationary-phase method or similarly the group-velocity concept (Lighthill 1965, 1978; Whitham 1973) can be applied to the far-field analysis. Its contribution features lee waves and their caustic, much as for the inertial waves in the homogeneous case. Most evanescent wave components contributing to ψ_2 attenuate exponentially in z except near $\omega = \sigma = 0$, where $|k|$ is also singular. This singularity, unaccounted for in the stationary phase method, will give rise to a large-scale cyclonic disturbance in the far field to be studied below.

5.2. *Three-dimensional far field* ($\hat{z} \gg 1$)

The contributions to the far field from ψ_1 and from ψ_2 will be analysed separately. Owing to the increasing rate of oscillation at large $\hat{z}$ in the phase $\hat{z}\Phi \equiv \omega x' + \sigma y + k\hat{z}$, the contribution of $h(\omega, \sigma)$ to ψ_1 of (5.5*a*) is generally small at a large distance, except in the neighbourhood of stationary points where $\partial\Phi/\partial\omega = \partial\Phi/\partial\sigma = 0$, i.e.

$$\left.\begin{aligned} \frac{\partial\Phi}{\partial\omega} &= X + \frac{\omega}{(\omega^2-\theta)^{\frac{1}{2}}(\omega^2+\sigma^2)^{\frac{1}{2}}}(2\omega^2+\sigma^2-\theta) = 0, \\ \frac{\partial\Phi}{\partial\omega} &= Y + \sigma\frac{(\omega^2-\theta)^{\frac{1}{2}}}{(\omega^2+\sigma^2)^{\frac{1}{2}}} = 0, \end{aligned}\right\} \tag{5.6}$$

where $X \equiv x'/\hat{z}$ and $Y \equiv y/\hat{z}$ are considered to be fixed. This gives four pairs of roots as stationary-point locations:

$$\omega_1 = \tfrac{1}{2}[k_+(|X|-u)]^{\frac{1}{2}}, \quad \sigma_1 = -\frac{k_+ Y}{\omega_1}; \quad \omega_2 = \tfrac{1}{2}[k_-(|X|+u)]^{\frac{1}{2}}, \quad \sigma_2 = -\frac{k_- Y}{\omega_2}, \tag{5.7a}$$

$$\omega_3 = -\omega_1, \quad \sigma_3 = -\sigma_1; \quad \omega_4 = -\omega_2, \quad \sigma_4 = -\sigma_2 \tag{5.7b}$$

where

$$u \equiv [X^2 - 8(Y^2+\theta)]^{\frac{1}{2}}, \quad k_\pm \equiv \tfrac{3}{4}|X| \pm \tfrac{1}{4}u.$$

As long as u is real, all ω_j and σ_j will be real, giving four stationary points for the integral ψ_1 for each point in the spatial domain $X^2 - 8(Y^2+\theta) > 0$. However, according to (5.6), X must be negative (corresponding to the downstream side), since $\omega^2 > \theta$ in ψ_1. Therefore the four real stationary points can exist only in

$$X < -2\sqrt{2}\,(Y^2+\theta)^{\frac{1}{2}}. \tag{5.8}$$

Thus the conic surface defined by the hyperbola $X = -2\sqrt{2}\,(Y^2+\theta)^{\frac{1}{2}}$ signifies a boundary, upstream of which prominent lee waves cannot be found. The appearance of θ in (5.8) shows clearly how the stratification rounds off the wedge-shaped leading edge of Lighthill's (1967) caustic and how it is displaced downstream. The hyperbolic caustic is illustrated in figure 2 (in dots) for three different values of θ, along with wave crests at $\hat{z} = 10$ computed as contours of constant phase.

The caustic represents the envelope of all the group-velocity vectors of the outgoing wavetrains. The limiting angle of these vectors in the far-field symmetry plane is precisely that specified by $X = -(8\theta)^{\frac{1}{2}}$ identifiable with the tilting angle of the caustic noted previously by Redekopp (1975).

5.2.1. ψ_1 *in the region downstream of the caustics*

The stationary points (ω_j, s_j) shown in (5.7) exist for this region. The inertial-wave-like mode ψ_1 is therefore dominated by the ranges of ω and σ around (ω_j, σ_j) which are the least affected by the self-averaging (destructive-interference) effect. Thus

$$\psi_1 \sim \pi \sum_{j=1}^{4} h(\omega_j, \sigma_j) \frac{e^{i\hat{z}\Phi(\omega_j, \sigma_j)}\, e^{\frac{1}{4}i\pi\,\mathrm{sgn}\,(A, B, C)_j}}{|A_j B_j - \frac{1}{4}C_j^2|^{\frac{1}{2}}\hat{z}}, \tag{5.9}$$

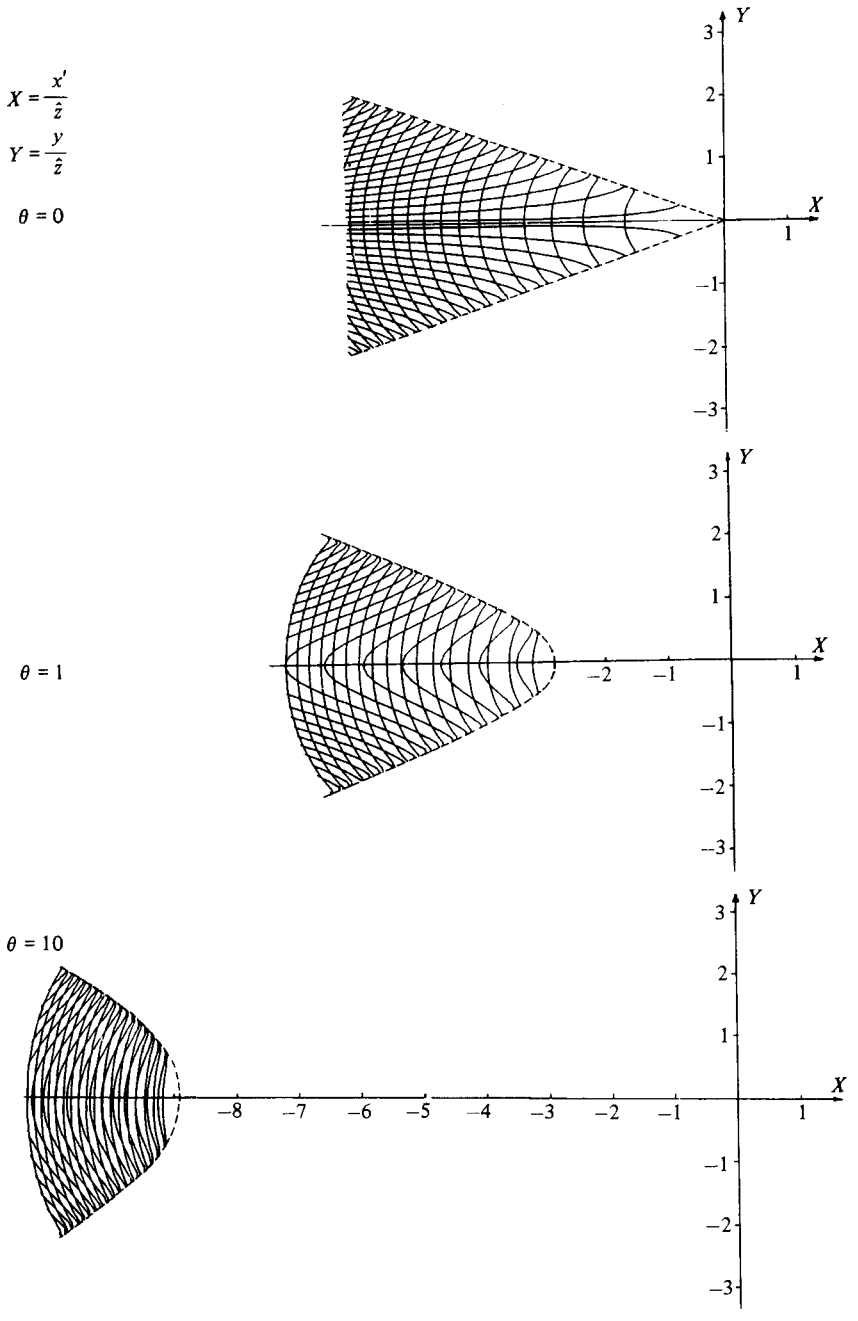

FIGURE 2. Wave crests and caustic at $\hat{z} = 10$ above a three-dimensional obstacle computed from far-field formulas for three values of stratification parameter $\theta = 0$, 1 and 10.

where A, B and C are $\frac{1}{2}\Phi_{\omega\omega}$, $\frac{1}{2}\Phi_{\sigma\sigma}$ and $\Phi_{\omega\sigma}$ respectively, and

$$\operatorname{sgn}(A,B,C)_j = \operatorname{sgn} A_j + \operatorname{sgn}\left(\frac{AB-\frac{1}{4}C^2}{A}\right)_j.$$

This can be more explicitly expressed, for fixed X, Y and θ, as

$$\psi_1 \sim \frac{1}{\pi\hat{z}|X^2-8(Y^2+\theta)|^{\frac{1}{4}}}\left\{\left|\frac{\omega_1^2-\theta}{k_+}\right|^{\frac{1}{2}} \operatorname{Re}[e^{i\hat{z}\Phi(\omega_1,\sigma_1)+\frac{1}{2}i\pi}F(\omega_1,\sigma_1)] - \left|\frac{\omega_2^2-\theta}{k_-}\right|^{\frac{1}{2}} \operatorname{Re}[e^{i\hat{z}\Phi(\omega_2,\sigma_2)}F(\omega_2,\sigma_2)]\right\}. \quad (5.10)$$

where Re signifies the real part,

$$i\hat{z}\Phi(\omega_1,\sigma_1) = -\tfrac{1}{2}i\hat{z}(\tfrac{3}{4}|X|+\tfrac{1}{4}u)^{\frac{3}{2}}(|X|-u)^{\frac{1}{2}},$$

and $i\hat{z}\Phi(\omega_2,\sigma_2)$ is the same except that u is now changed to $-u$. The other factors in (5.10) involving $k_\pm$ and $\omega_{1,2}$ may also be written as

$$|(\omega_1^2-\theta)/k_+|^{\frac{1}{2}} = |[(|X|-k_+)^2+Y^2]/k_+|^{\frac{1}{2}},$$

and $|(\omega_2^2-\theta)/k_-|^{\frac{1}{2}}$ are the same except that k_+ is now changed to k_-. In the limit $\theta\to 0$ (5.10) recovers precisely the far-field expression for ψ in the unstratified case corresponding to that of the w in Cheng & Johnson (1983).

At larger θ the wave pattern behind the caustic determined by ψ_1 remains similar to that at $\theta = 0$, except that the region delimited by $X+[8(Y^2+\theta)]^{\frac{1}{2}} < 0$ is to be found downstream at a larger X, and that the wavenumber level increases with θ like $\hat{z}\theta$. However, the amplitude for ψ_1 must greatly diminish with increasing θ, since $F(\omega,\sigma)$ vanishes with increasing ω and σ. Equation (5.10) indicates explicitly how ψ_1 in the far field is controlled by the vertical distance $\hat{z}$ and the distance from the caustic. The unbounded singularity at $X = -2[2(Y^2+\theta)]^{\frac{1}{2}}$ confirms the breakdown of (5.10) near the caustic, which is to be anticipated since it corresponds to the vanishing of the stationary-phase expansion's discriminant (cf. (5.9)). Therefore a development for large $\hat{z}$ must be carried out separately for the vicinity of the caustic.

5.2.2. ψ_1 *in the caustic transition zone*

Near the caustic the four narrow ranges of ω and σ contributing effectively to ψ merge into two ranges around

$$(\omega,\sigma) = (\tfrac{1}{4}\sqrt{3}\,|X|, -\sqrt{3}\,Y) \quad \text{and} \quad (\omega,\sigma) = (-\tfrac{1}{4}\sqrt{3}\,|X|, \sqrt{3}\,Y). \quad (5.11)$$

It is expedient to introduce a small variable r to replace X, and small frequency parameters λ and Q to replace ω and σ:

$$X^2 = 8(Y^2+\theta)(1+r), \quad \omega^{\pm} = \pm\tfrac{1}{2}\sqrt{3}\,(Y^2+\theta)^{\frac{1}{2}}(1+\lambda), \quad \sigma^{\pm} = \mp\sqrt{3}\,Y(1+Q-2\lambda), \quad (5.12)$$

where the superscripts + and − refer to the positive and negative ranges of ω; the variable r is positive on the downstream side and negative on the upstream side. The Φ may then be developed for small r, λ and Q, considering first a positive ω,

$$\Phi \sim -\tfrac{1}{16}\sqrt{3}\,X^2(3-r) - \tfrac{1}{8}\sqrt{3}\,X^2r\lambda + \tfrac{1}{2}\sqrt{3}\,Y^2(Y^2+\theta)(3Y^2+\theta)^{-1}Q^2 + \tfrac{3}{8}\sqrt{3}\,X^2\lambda^3 + \ldots. \quad (5.13)$$

Notice the absence of terms proportional to λ or Q at $r = 0$. The Φ for a negative ω has the same development except for an algebraic sign. The results may be expressed as

$$\psi_1 \sim 2\,\mathrm{Re}\,\psi_1^+ \sim \mathrm{Re}\left\{\frac{\mathrm{i}}{\pi^{\frac{1}{2}}3^{\frac{7}{12}}}\frac{(X^2+16\,Y^2)^{\frac{1}{2}}}{\sqrt{2}\,|X|^{\frac{3}{2}}\hat{z}^{\frac{5}{6}}}F(\tfrac{1}{4}\sqrt{3}\,|X|,-|3\,Y|^{\frac{1}{2}})\right.$$
$$\left.\times\,\mathrm{Ai}\,(\zeta)\exp\left[-\mathrm{i}\tfrac{3}{16}\theta^{\frac{1}{2}}X^2\hat{z}(1-\tfrac{1}{3}r)+\tfrac{1}{4}\mathrm{i}\pi\right]\right\} \quad (5.14)$$

where $\mathrm{Ai}\,(\zeta)$ is the Airy integral and ζ rescaled r:

$$\mathrm{Ai}\,(\zeta) = \frac{1}{2\pi}\int_{-\infty}^{\infty} \mathrm{e}^{\mathrm{i}(\frac{1}{3}t^3+\zeta t)}\,\mathrm{d}t, \quad \zeta \equiv -\frac{|X|^{\frac{4}{3}}}{3^{\frac{1}{3}}4}\hat{z}^{\frac{2}{3}}r.$$

Note that the X^2 in the imaginary exponential argument of (5.14) is $X^2 = 8(Y^2+\theta)$. As $r\to-\infty$, ψ_1 of (5.14) matches that of (5.10) from the downstream. As $r\to+\infty$, it yields an exponential decay upstream. Higher-order contributions unaccounted for in the above analysis will decide the correct algebraic decay to match that in the upstream region.

5.2.3. ψ_1 *upstream of the caustic*

There is no stationary point in (ω, σ) for (X, Y) upstream of the caustic. Examination for a fixed X, Y and θ shows that ψ_1 in this region decays with increasing height no slower than $\hat{z}^{-3}$ upstream of the caustic. A similar conclusion for ψ_1 also holds for an unbounded θ for $\theta\hat{z} \gg 1$, which is found to be comparable to $\theta F(\theta^{\frac{1}{2}}, 0)/(\theta\hat{z})^3$. For $\theta \ll 1$ the far-field estimates for ψ_1 must take into account the relative magnitudes of θ^{-1} and $\hat{z}$. In the limit $\theta\to 0$ the corresponding result of Cheng (1977) is recovered.

5.2.4. *Contribution from* ψ_2

It is essential to recall that the far-field behaviour in the three distinct regions of §§5.2.1–5.2.3 are significant only with regard to ψ_1, i.e. the contribution from the outgoing wave components. However, the contribution from the evanescent wave components ψ_2 will be seen to be equally or more important, unless $\theta = 0$. The evanescent components generally attenuate at an exponential rate. Hence they are unimportant in the far field, but exceptions occur in vicinities of singularities where the imaginary part of the phase $\hat{z}\Phi$ also vanishes. This happens at $\omega = \sigma = 0$ in the present problem. The following analysis for ψ_2 therefore represents an amendment of the stationary-phase or saddle-point method.

To analyse the latter behaviour we recast the integral of ψ_2 of (5.5*b*) into polar representation with $\rho \equiv (\omega^2+\sigma^2)^{\frac{1}{2}}$, $\vartheta = \tan^{-1}(\sigma/\omega)$,

$$\psi_2 = -\int_0^{2\pi}\frac{\mathrm{d}\vartheta}{(2\pi)^2}\int_0^{\theta^{\frac{1}{2}}\sec\vartheta} F((\rho,\vartheta))\,(\theta-\rho^2\cos^2\vartheta)^{\frac{1}{2}}$$
$$\times\exp\{[\mathrm{i}(X\cos\vartheta+Y\sin\vartheta)-(\theta-\rho^2\cos^2\vartheta)^{\frac{1}{2}}]\rho\hat{z}\}\,\mathrm{d}\rho, \quad (5.15)$$

where $F((\rho,\vartheta)) = F(\omega,\sigma)$. The real exponent $-\rho\hat{z}(\theta-\rho^2\cos^2\vartheta)^{\frac{1}{2}}$ shows exponential decay for all ϑ and ρ, except at $\rho = 0$ and at $\rho = \theta^{\frac{1}{2}}\sec\vartheta$, where the imaginary part of the phase $\hat{z}\Phi$ is seen to be both zero and singular in the (ω,σ)-domain. The integral over ρ may, however, be evaluated by parts. If we retain only the lowest-order term in $(\theta\hat{z})^{-1}$, the integral in question is

$$-\frac{F((0,\vartheta))\,\theta^{\frac{1}{2}}}{\hat{z}[\mathrm{i}(X\cos\vartheta+Y\sin\vartheta)-\theta^{\frac{1}{2}}]}.$$

Note that the upper limit at $\rho = \theta^{\frac{1}{2}} \sec\vartheta$ does not contribute, owing to the presence of the factor $(\theta - \rho^2\cos^2\vartheta)^{\frac{1}{2}}$ in (5.15). Therefore, subject to a relative error of order $(\theta\hat{z})^{-1}$, one arrives at

$$\psi_2 \sim -\frac{F(0,0)}{(2\pi)^2\,\hat{z}} \int_0^{2\pi} \frac{\mathrm{d}\vartheta}{1 - \mathrm{i}(X\cos\vartheta + Y\sin\vartheta)}, \tag{5.16a}$$

or

$$\psi_2 \sim -\frac{F(0,0)}{2\pi\hat{z}[1 + (X^2+Y^2)/\theta]^{\frac{1}{2}}}, \tag{5.16b}$$

where $F(0,0)$ is identified simply as the normalized displaced volume of the obstacle.

Unlike that of ψ_1, which has a bias in the downstream direction for all θ, the contribution of ψ_2 is centred around the vertical $\hat{z}$-axis directly above the obstacle; except for a scale change in the coordinates, it has the same effect of a point source on the velocity potential in classical hydrodynamics. The region upstream of the caustic, where the lee wave from ψ_1 is absent, is therefore dominated by ψ_2, which according to (5.16) is of order $1/\hat{z}$. Therefore it is comparable to the magnitude of ψ_1 behind the caustic. Its relative importance will be further increased for a large θ, not only because the horizontal scale of the field is increased by the factor $\theta^{\frac{1}{2}}$, but also because the typical magnitude of ψ_2 upstream of the caustic and that of the lee waves of ψ_1 downstream of the caustic is in the proportion of $F(0,0) : F(\sqrt{\theta}, 0)$, noting that $F(\omega, 0)$ vanishes for $|\omega| \to \infty$.

In contrast with the lee-wave pattern of ψ_1, in which wave crests are densely packed, the symmetrically distributed pressure compression given by (5.16) (recalling $p = -2\psi$) implies an anticyclonic disturbance, causing a clockwise twist of streamlines in a horizontal plane for a positive $F(0,0)$ and a cyclonic one with a counterclockwise twist for a negative $F(0,0)$. This makes possible at a large enough θ the occurrence of a trapped-fluid region above the obstacle, suggesting a deformed Taylor column (cf. §4.3, also Hide 1971).

The result (5.16) may not be too surprising in view of the development in §4 for large θ, since the source-like behaviour shown is a particular solution to the Laplace equation. The interesting, unsuspected feature is its coexistence with the lee-wave mode ψ_1 and its omnipresence for all $\theta \neq 0$. As θ decreases toward zero, its horizontal scale diminishes and the domain $(X^2+Y^2)^{\frac{1}{2}} = O(\theta^{\frac{1}{2}})$ for ψ_2 along with the leading edge of the caustic merges into the neighbourhood of the vertical axis from the obstacle. Its amplitude however, remains unchanged.

5.3. *Two-dimensional solution and far field*

For a two-dimensional ridge-type topography, the Fourier integral of ψ does not exist for an unbounded Θ in the Riemann sense, owing to the pole singularity in h. One could nevertheless define the solution ψ via a contour integral. We choose, however, to analyse first the velocity field, in particular $\partial\psi/\partial x'$, for which the solution may again be obtained as the sum of two distinct terms:

$$\frac{\partial}{\partial x'}\psi = \frac{\partial}{\partial x'}\psi_1 + \frac{\partial}{\partial x'}\psi_2, \tag{5.17}$$

with

$$\frac{\partial\psi_1^{\pm}}{\partial x'} \equiv -\int_{\pm\theta^{\frac{1}{2}}}^{\pm\infty} \frac{F(\omega)}{2\pi} |\omega^2 - \theta|^{\frac{1}{2}} \exp\{\mathrm{i}[\omega x' + \omega\,|\omega^2 - \theta|^{\frac{1}{2}}\hat{z}]\}\,\mathrm{d}\omega,$$

$$\frac{\partial\psi_2^{\pm}}{\partial x'} \equiv \mp\mathrm{i}\int_0^{\pm\theta^{\frac{1}{2}}} \frac{F(\omega)}{2\pi} |\omega^2 - \theta|^{\frac{1}{2}} \exp\{\mathrm{i}\omega x' - |\omega|\,|\omega^2 - \theta|^{\frac{1}{2}}\hat{z}\}\,\mathrm{d}\omega.$$

The far-field expression for the two parts of (5.17) may be carried out in a manner similar to §5.2. The evanescent components in this case contribute as

$$\frac{\partial \psi_2}{\partial x'} \sim -\frac{F(0)\,(X/\theta^{\frac{1}{2}})}{\pi \hat{z}(1+X^2/\theta)}, \tag{5.18a}$$

from which ψ_2 is seen to be

$$\psi_2 \sim -\frac{F(0)}{2\pi} \ln \left| \frac{x'^2}{\theta} + \hat{z}^2 \right|, \tag{5.18b}$$

assuming $\partial \psi_2/\partial \hat{z}$ to vanish as $|x'| \to \infty$. The vertical velocity w and the streamline deflection in this case can be similarly worked out, but their magnitude is much weaker, as already noted. We note that, in the two-dimensional problems, the lee-wave caustic for ψ_1 is $X = -(8\theta)^{\frac{1}{2}}$ and that the lee-wave amplitude from ψ_1 is typically of order $\theta^{\frac{1}{2}} F(\theta^{\frac{1}{2}})\, \hat{z}^{-\frac{1}{2}}$.† From (5.17), the drag of a mountain ridge can be evaluated. We note in passing that Smith (1979*a*) has analysed a similar two-dimensional ridge problem for a high $\mathscr{R}$, including the $O(\mathscr{R}^{-1})$ correction on the mountain drag.

6. Examples: computation and study for moderate and high $\hat{z}$

In the following, we discuss numerical examples of two- and three-dimensional solutions which are computed with the help of the fast Fourier transform (FFT). Mainly the results for smooth topography $Z_w = (1+x'^2)^{-1}$ and $Z_w = (1+x'^2+y^2)^{-2}$ at reduced height $\hat{z}$ ranging from 2 to 15 are studied. Against these data, the analytical far-field results of §5.2 will be compared, and the importance of the cyclonic feature is verified.

6.1. *Use of the FFT algorithm*

The FFT algorithm employs typically 1024 uniform divisions over the ω-range $[-32\pi, 32\pi]$ and over the x-range $[-16, 16]$ for two-dimensional problems; in the three-dimensional cases 1024 uniform divisions over $-16\pi < \omega < 16\pi$ and 64 over $-\pi < \sigma < \pi$ are used. The mesh spacings are typically $\Delta\omega = \Delta\sigma = 2\pi/64$, with $\Delta X = \frac{1}{16}$, $\Delta Y = \frac{1}{2}$. We note that a sufficiently fine mesh in (ω, σ) is needed near $\omega = \sigma = 0$ to resolve the singularity $(\omega^2-\theta)^{\frac{1}{2}}/(\omega^2+\theta^2)^{\frac{1}{2}}$ in the three-dimensional solution; cf. (5.4) or (5.5). In addition, an even finer mesh is required to recover accurately the pressure hill of ψ_2 (see §6.3 below). On the other hand, with a fixed number of divisions assigned to ω and σ, a finer uniform mesh means reductions in the upper limits on ω and σ, therefore a loss in the ability to resolve the finer field structures. The choice of $\Delta\omega = \Delta\sigma = 2\pi/64$ represents a compromise. The mesh divisions in X and Y define the locations at which the solution data are available. Their relatively large sizes do not affect the truncation errors.

6.2. *Two-dimensional examples*

Figure 3 presents the spanwise velocity $\partial\psi/\partial x'$ at $\hat{z} = 5$ as a function of X for a ridge topography $Z_w = (1+x'^2)^{-1}$ at two levels of stratification, $\theta = 1$ and $\theta = 5$. The FFT solution for $\partial\psi/\partial x'$ at $\theta = 1$ and $\hat{z} = 5$ in figure 3(*a*) shows clearly the densely packed lee-wave pattern behind the caustic, $X < -(8\theta)^{\frac{1}{2}}$, as in the unstratified case. Superimposed on the latter is a doublet-like antisymmetrically distributed $\partial\psi/\partial x'$ as anticipated from the preceding far-field study (5.18*a*). A few precursor wavelets are noticeable over $-(8\theta)^{\frac{1}{2}} < X < 0$, which may be attributed to the transitional

† For a narrow ridge of finite span, one must allow in (5.18) a correction to the relative wind velocity due to a self-induced velocity pertaining to a three-dimensional correction (cf. Cheng *et al.* 1982, p. 18). This point has also been observed by Smith (1979*b*).

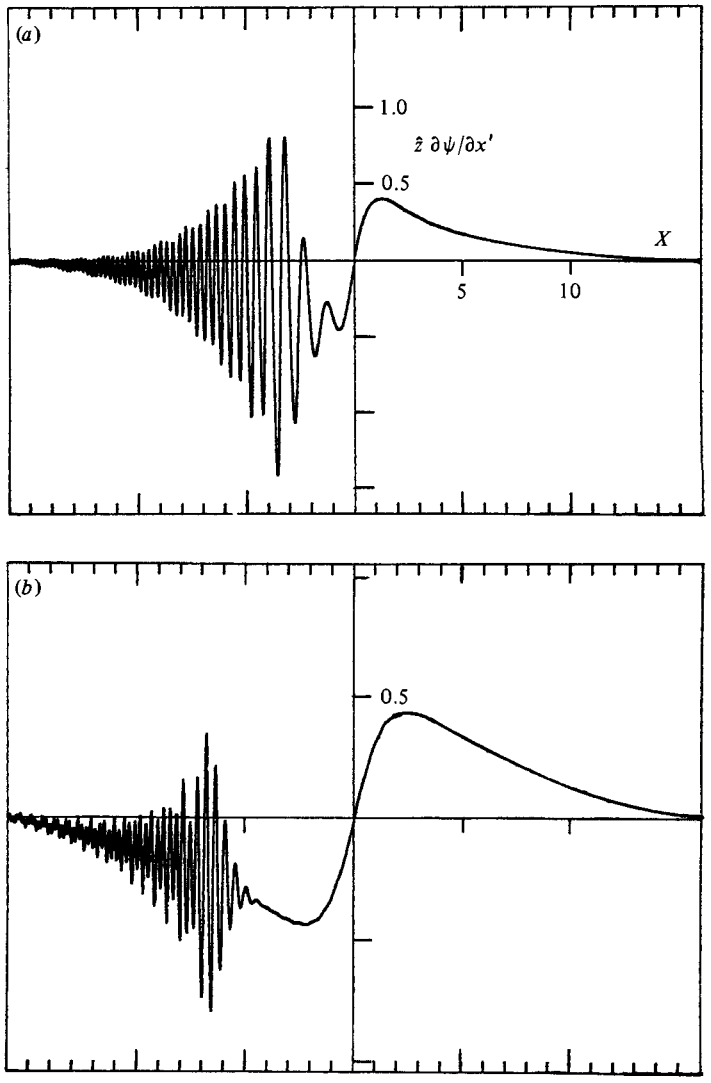

FIGURE 3. Horizontal velocity perturbation as a function of X above the two-dimensional ridge $Z_w = (1+x'^2)^{-1}$ at $\hat{z} = 5$ for two degrees of stratification: (*a*) $\theta = 1$, (*b*) $\theta = 5$. $\Delta\omega = 2\pi/32$, $N = 1024$.

structure of the caustic zone (with a thickness perhaps of the order $\hat{z}^{-\frac{2}{3}}$). The peak in the lee-wave amplitude appears to be comparable to, but noticeably larger than, that of the smooth doublet-like mode upstream ($X > 0$). This is understandable from comparison of the magnitude of $\partial\psi_1/\partial x'$ to that of $\partial\psi_2/\partial x'$. The former is of order $\theta^{\frac{1}{4}}F(\theta^{\frac{1}{2}})/|\hat{z}|^{\frac{1}{2}}$, and the latter belongs to the order $\theta^{\frac{1}{2}}F(0)/|\hat{z}|$. Thus, increasing the height should enhance the relative prominence of the lee-wave group (in the spanwise velocity) over a ridge, while increasing stratification has the opposite effect. These expectations are quite clearly substantiated by the result obtained for a higher elevation $\hat{z} = 10$ (not shown) and by figure 3(*b*), where θ is increased to 5 for $\hat{z} = 5$. Note that the peak of the lee-wave group in figure 3(*b*) is shifted to a considerable distance downstream close to $X = -(8\theta)^{\frac{1}{2}} = -\sqrt{40}$. Also note that the lee waves in figure 3(*b*) are more densely packed than those in figure 3(*a*). It may be explained by the increased magnitude of the imaginary argument in $e^{i\Phi\hat{z}}$.

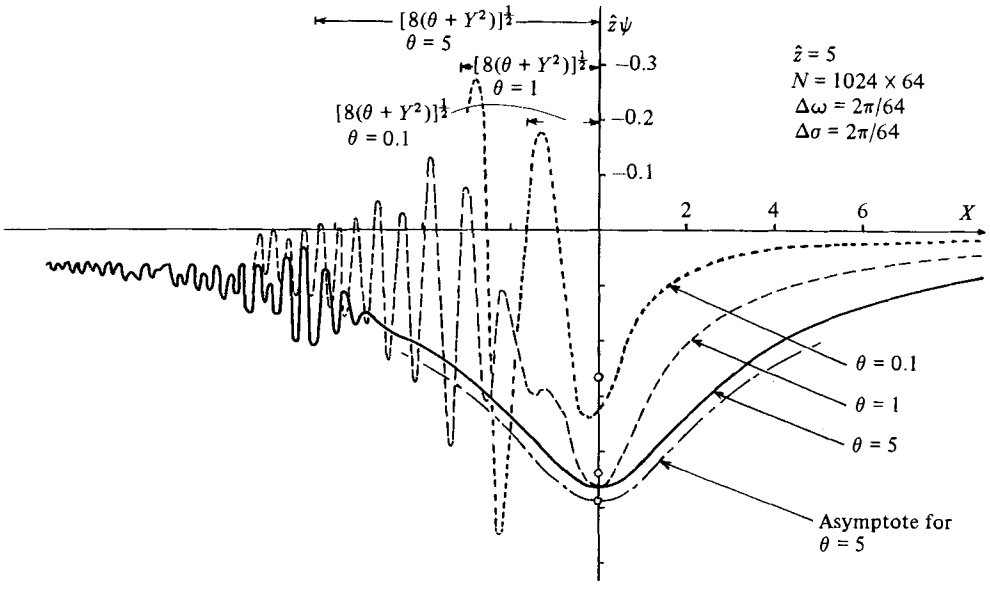

FIGURE 4. Distribution of $\hat{z}\psi$ as a function of X along $Y = 0.5$ for three different degrees of stratification: $\theta = 0.1$, 1 and 5. The obstacle shape is $Z_w = (1+x'^2+y^2)^{-2}$. $\hat{z} = 5$, $N = 1024 \times 64$, $\Delta\omega = 2\pi/64$, $\Delta\sigma = 2\pi/64$.

It is essential to recall that the source-like logarithmic behaviour of the pressure field given by (5.18*b*) would dominate over the corresponding lee-wave pressure even for a moderate $\theta = 1$ at $\hat{z} = 5$. On the other hand, one would find little evidence of the evanescent components in the upwash w, or of the upward streamline displacement, as explained earlier at the end of §4. (Figure 5 in Cheng *et al.* (1982) illustrates the vertical velocity computed by the FFT technique for $\hat{z} = \theta = 5$.)

6.3. *Three-dimensional examples*

We study next the numerical examples of three-dimensional solutions (5.4) via the FFT technique, considering a smooth shape $Z_w = (1+x'^2+y^2)^{-2}$ for which $F(\omega, \sigma) = \pi\rho K_1(\rho)$, where $\rho \equiv |\omega^2+\sigma^2|^{\frac{1}{2}}$ and $K_1(\rho)$ is the Bessel function of the second kind of the first order. To illustrate the prominence of the cyclonic feature and how the stratification controls the far-field structure, the pressure distributions along a horizontal line $Y = 0.5$ and $\hat{z} = 5$ are presented in figure 4 in the form of $\hat{z}\psi$ versus X, for three levels of stratification, $\theta = 0.1$, 1 and 5. The termination of ω at $\pm 16\pi$ is expected to cause inaccuracy in defining the refined structure of the wave group, but is quite adequate for describing the pressure hill of interest.

Several features in good agreement with the far-field analysis of §5.2 are apparent from figure 4: (i) the wavenumber intensity increases with θ; the wave packets diminish in strength with θ, being shifted downstream by an amount roughly $(8\theta)^{\frac{1}{2}}$ at their leading edges; (ii) distinct from, and superimposed upon, the wave pattern is the smoothly distributed depression (negative) of ψ corresponding to the 'pressure hill' (recall $p = -2\psi$), which extends symmetrically about a vertical axis above the obstacle, thereby raising the *mean* level of the lee-wave pressure above zero (or lowering the mean ψ level below zero); (iii) the horizontal scale of the 'hill' increases and decreases with θ, but one cannot find in any case its peak reducing rapidly with a decreasing θ (including the case $\theta = 0.1$ shown). If one takes into account the

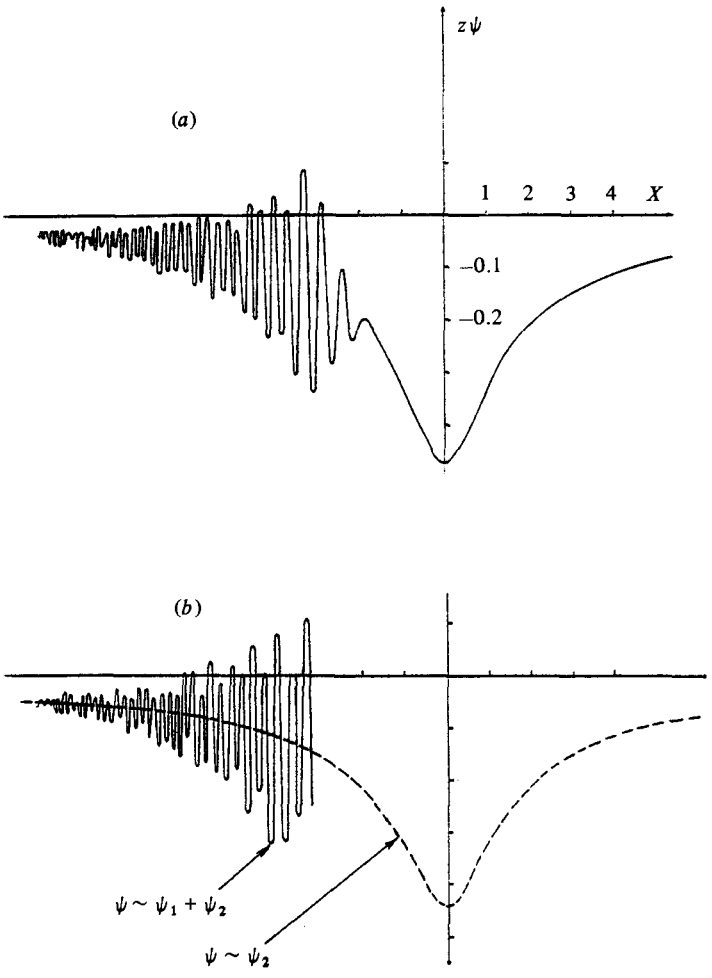

FIGURE 5. Details of solution structure computed from FFT algorithm and from asymptotic analyses for $\theta = 1$, $\hat{z} = 10$ and $Y = 0.5$: (*a*) FFT; (*b*) asymptotic. The obstacle shape is $Z_w = (1 + x'^2 + y'^2)^{-2}$. $N = 1024 \times 64$, $\Delta\omega = 2\pi/64$, $\Delta\sigma = 2\pi/64$.

different θ-values and the fact that $Y = 0.50 \neq 0$, one finds the asymptotic value of $\min(\hat{z}\psi)$ from (5.16) to be -0.488, -0.447 and -0.267 for θ equal to 5, 1 and 0.1 respectively (shown as open circles). They are indeed not far away from the corresponding FFT data curves. A more detailed study shows that the correlation with the pressure hill should improve not only with increasing height $\hat{z}$, but also with increasing stratification θ.

We note that the $\hat{z}\psi$ data of $\hat{z} = 5$ for $\theta = 1$ in figure 4 agree exceedingly well with the asymptotic formula (5.16). The correlated data for the higher stratification ($\theta = 5$) agree also quite well with (5.16); however, slight discrepancies are discernible which indicates a limitation of the FFT algorithm in use and are traceable to the discretization errors in the (ω, σ)-domain. With these considerations taken into account, the singularities in (5.15) suggest that the FFT results obtained may not be very accurate for $\hat{z} > 10$, and, perhaps, $\theta > 5$.

To ascertain further the quality of the computation and the adequacy of the asymptotic analysis, we show in figure 5(*a*) the detailed distributions of ψ at $\hat{z} = 10$ and $Y = 0.5$ for $\theta = 1$ from the FFT integration with $\Delta\omega = \Delta\sigma = 2\pi/64$, and we

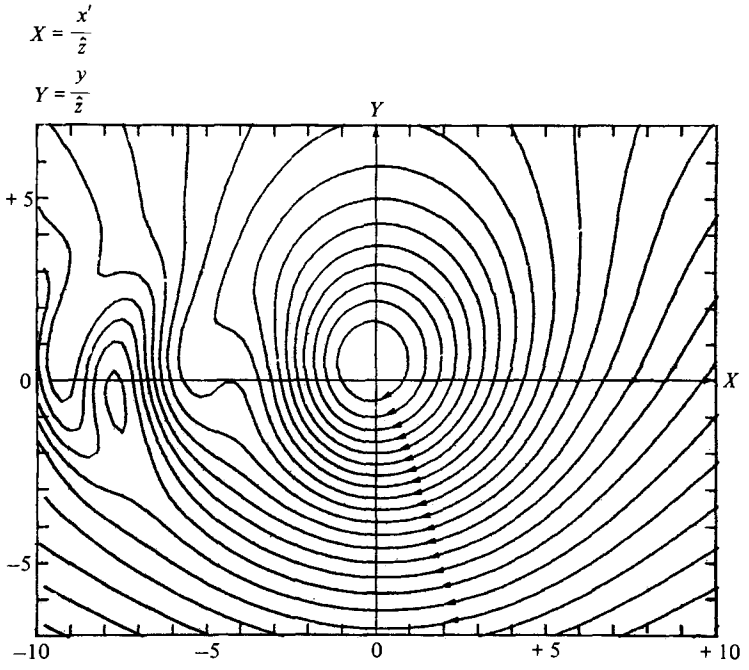

FIGURE 6. Horizontal streamline pattern above the obstacle $z_w/L = \tau/(1+x'^2+y^2)^2$ at a mid-altitude $\hat{z} = 0.50$ under a stratification $\theta = 5$; $\tau = 0.25$.

compare it with the corresponding far-field results $\psi = \psi_1 + \psi_2$, based on (5.10) and (5.16), where the detail is shown in figure 5(*b*). Both the pressure hill from (5.16) and the lee-wave pattern from (5.10) as well as the leading edge of the wave pack are reproduced and marked in figure 5(*b*). Evidently the mesh with $\Delta\omega = \Delta\sigma = 2\pi/64$ is sufficient for capturing most of the far-field features of interest for this case of $\theta = 1$. The fine pattern of lee waves behind the caustic in the two plots appears to correspond rather closely; point-by-point comparison is impossible unless the range of ω and σ can be further increased. One notes that the existence of two distinct rapidly oscillating modes, cf. (5.10), causes the lee-wave envelope to be ill-defined. Therefore, the asymptotic envelope is not shown in the three-dimensional study.

Finally, we show in figure 6 a horizontal streamline pattern from the FFT solution for $\theta = 5$ at a mid-altitude $\hat{z} = 0.50$. An obstacle thickness ratio $\tau = 0.25$ is assumed, giving a sizable $\tau\theta^2 = 0.56$. It is stipulated in the calculation that the trapped fluid inside the closed streamsurface also originates from the same uniform state. The pattern confirms the existence of a column-like closed streamsurface, revealing also stationary eddies in the lee in this case. The latter is evidently an inertial-wave correction to the geostrophic/hydrostatic-balance model discussed in §4. Flow patterns for other combination of τ and θ are presented along with data for a non-vanishing $\mathscr{R}$ in a forthcoming paper.

7. Concluding remarks

The foregoing study shows that an obstacle or the topography at the horizontal base of a stably stratified, deep, rotating fluid supports not only lee waves at great (scaled) height, which depends critically on the surface geometry, but also a high- or low-pressure region associated with a cyclonic disturbance in the far field, which

depends only on the obstacle displacement volume. Except in the homogeneous limit ($\theta = 0$), this cyclonic feature exists at all degrees of stratification, but has not been taken into account in existing far-field studies based on the group-velocity concept or stationary-phase method. The limit of an unbounded θ in the present work recovers the Laplace equation with the Neumann boundary condition of Hogg (1973) and Ingersoll (1969), in which a solitary anticyclonic disturbance in the far field is implicit and is responsible for the large-scale stationary eddy at a high θ. The coexistence of a solitary cyclonic disturbance with lee waves in the far field at all bounded $\theta \neq 0$ has never been suspected, however. Although the analysis presented are limited to a small $\mathscr{R}$, the cyclonic feature will also remain for all $\mathscr{R} \neq \infty$ as an examination of the contribution from the evanescent wavetrain at $\omega = \sigma = 0$ for $\mathscr{R} \neq 0$ will readily confirm in the linear case.

Our basic mathematical model is that of an inviscid Boussinesq fluid in almost-rigid-body rotation about a vertical axis. Thus, unlike models of planetary atmospheres and oceans, the theory can be subjected to laboratory verification in an upright rotating container. Both the far-field analysis and the computational studies have been based on the solution to the linearized version of the reduced equations of the asymptotic theory appropriate for a *thin* obstacle, which is further specialized to an infinite depth. The results are expected to furnish a meaningful characterization of the flow and wave patterns of a rapidly rotating Boussinesq fluid, *not* necessarily restricted to a thin topography, since the linearization does not lead to a degeneracy. The linear solution provides a valuable base for testing and guiding computation methods for the study of the corresponding nonlinear problem.

Among the outstanding questions raised by the cyclonic far field are one on its evolution and another on the admissibility of a periodic solution as an alternative to the steady-state solution at large t. Their answers, even in the framework of the linear theory, should be of great interest to an understanding of the cyclogenesis (cf. discussions in Buzzi & Tibaldi 1977; Hogg 1980).

The analysis for a non-vanishing Rossby number, to appear in a forthcoming paper, will complement the present work and bring out the subtle alterations in the flow structure related to changes in the group-velocity direction at $\theta < (\frac{1}{2}\mathscr{R})^{-2}$ to that at $\theta > (\frac{1}{2}\mathscr{R})^{-2}$. This changeover will affect critically the wave patterns about, as well as the hydrodynamic forces on, a ground topography. The Earth's rotation effects on (stratified) flows over mountains, particularly on drags and side forces of ridges, have been studied in a series of highly interesting papers by Smith (1979*a*, *b*, *c*), as noted earlier. Smith's analysis are restricted to cases corresponding to either a very large $\mathscr{R}$ or a very small $\mathscr{R}$; the existence of the critical condition $\mathscr{R}^2\theta = \frac{1}{4}$ was not considered.

An important aspect not considered above is the viscous effects. From Johnson's (1982) study, it is seen that viscous damping and the Eckman-layer pumping have the expected effect of reducing the high-wavenumber components. Since the wavenumber intensity in the lee waves increases with θ, according to the foregoing inviscid analysis, the expected viscous dissipation of the lee waves should further enhance the prominence of the cyclonic feature. Another important aspect yet to be studied is the effect of a finite depth. Stewartson & Cheng (1979) found that the homogeneous flow in a rotating container supports a bimodal structure, of which one mode is columnar in character and is controlled by $\Theta^{-1} = L/\mathscr{R}H$. The latter mode is absent in the solution for an infinite depth, and its significance appears to be substantiated by laboratory study (Heikes & Maxworthy 1982). The occurrence of this as well as the feature corresponding to the cyclonic disturbance in the case of finite Θ and $\theta \neq 0$ remain to be confirmed.

We dedicate this work to the late Professor Keith Stewartson, whose advice and friendship have been a constant source of enlightenment. We would like to thank Drs E. R. Johnson, R. H. Edwards, L. G. Redekopp and K. Heikes for valuable discussions on related studies. The research was supported by the United States National Science Foundation, Engineering Division under Grant CME-7822075.

REFERENCES

BATCHELOR, G. K. 1967 An *Introduction to Fluid Dynamics*, p. 567. Cambridge University Press.

BLUMEN, W. 1972 *Rev. Geophys. Space Phys.* **10**, 485.

BUZZI, A. & TIBALDI, S. 1977 *Q. J. R. Met. Soc.* **103**, 135.

CHENG, H. K. 1977 *Z. angew. Math. Phys.* **28**, 753.

CHENG, H. K. & JOHNSON, E. R. 1982 *Proc. R. Soc. Lond.* A **383**, 71.

CHENG, H. K., HEFAZI, H. & BROWN, S. N. 1982 *Univ. S. Calif. School Engng, Aerospace Engng Dept Rep. USCAE* 140.

ECKART, C. 1960 *Hydrodynamics of Ocean and Atmosphere.* Pergamon.

GREENSPAN, H. P. 1969 *The Theory of Rotating Fluids*, p. 51. Cambridge University Press.

HEIKES, K. E. & MAXWORTHY, T. 1982 *J. Fluid Mech.* **125**, 319.

HIDE, R. 1971 *J. Fluid Mech.* **49**, 745.

HIDE, R., IBBETSON, A. & LIGHTHILL, M. J. 1968 *J. Fluid Mech.* **32**, 251.

HOGG, N. G. 1973 *J. Fluid Mech.* **58**, 517.

HOGG, N. G. 1980 Effects of bottom topography on ocean currents. In *Orographic Effects in Planetary Flows; GARP Publ. Series* **23**, 169.

HUPPERT, H. E. 1975 *J. Fluid Mech.* **67**, 397.

INGERSOLL, A. P. 1969 *J. Atmos. Sci.* **26**, 744.

JOHNSON, E. R. 1978 *J. Fluid Mech.* **86**, 209.

JOHNSON, E. R. 1982 *J. Fluid Mech.* **120**, 359.

LIGHTHILL, M. J. 1965 *J. Inst. Math. Appl.* **1**, 1.

LIGHTHILL, M. J. 1967 *J. Fluid Mech.* **27**, 725.

LIGHTHILL, M. J. 1978 *Waves in Fluids.* Cambridge University Press.

MAXWORTHY, T. 1977 *Z. angew. Math. Phys.* **28**, 853.

OBUKHOV, A. M. 1949 *Izv. Akad. Nauk SSSR Ser. Geograf.-Geofiz.* **13**, 281. (English transl. Dept Meteorol., Univ. Chicago).

OGURA, Y. & PHILLIPS, W. A. 1962 *J. Atmos. Sci.* **19**, 173.

QUENEY, P. 1948 *Bull. Am. Meteor. Soc.* **29**, 16.

REDEKOPP, L. G. 1975 *Geophys. Fluid Dyn.* **6**, 289.

SMITH, R. 1979*a* *J. Atmos. Sci.* **36**, 177.

SMITH, R. 1979*b* *J. Atmos. Sci.* **36**, 2395.

SMITH, R. 1979*c* *Adv. Geophys.* **21**, 87.

STEWARTSON, K. & CHENG, H. K. 1979 *J. Fluid Mech.* **91**, 415.

STIX, T. H. 1962 *The Theory of Plasma Waves*, p. 13. McGraw-Hill.

WHITHAM, G. B. 1973 *Linear and Nonlinear Waves.* Wiley.

YIH, C. S. 1965 *Dynamics of Nonhomogeneous Fluids.* Macmillan.

YIH, C. S. 1978 *Fluid Dynamics.* West River.